



Tissue engineering approach to the creation of grafting material for rhinoplasty: clinical case reports

Vladimir Karpiuk^{1,2*} , Irina Gilevich¹ , Marina Perova³ , Olga Ponkina⁴ 

¹Laboratory for Development and Study of New Treatment Technologies, Prof. S. V. Ochapovsky Research Institute-Regional Clinical Hospital No. 1, 350086 Krasnodar, Russia

²Department of Plastic Surgery, Chalet Sante Clinic, 350020 Krasnodar, Russia

³Department of Surgical Dentistry and Maxillofacial Surgery, Kuban State Medical University, 350063 Krasnodar, Russia

⁴Pathology Department, Prof. S. V. Ochapovsky Research Institute-Regional Clinical Hospital No. 1, 350086 Krasnodar, Russia

***Correspondence:** Vladimir Karpiuk, Department of Plastic Surgery, Chalet Sante Clinic, 238 Krasnykh Partizan street, 350020 Krasnodar, Russia. vkarpyuk@mail.ru

Academic Editor: Diego Mantovani, Laval University, Canada

Received: September 19, 2023 **Accepted:** March 3, 2024 **Published:** June 3, 2024

Cite this article: Karpiuk V, Gilevich I, Perova M, Ponkina O. Tissue engineering approach to the creation of grafting material for rhinoplasty: clinical case reports. *Explor BioMat-X*. 2024;1:158–73. <https://doi.org/10.37349/ebmx.2024.00011>

Abstract

The use of autologous cartilage and bone grafts remains the gold standard in augmentation rhinoplasty performed to reconstruct of the nasal dorsum. Meanwhile, limited number of available sources, donor site morbidity, and unpredictable graft resorption represent significant disadvantages of autografting. The aim of this study is to test combination of autologous stromal vascular fraction (SVF) and commercially available bone substitutes (BSs) as new tissue-engineered grafting material (GM) for rhinoplasty. A series of consecutive cases includes four adult patients who underwent rhinoplasty to correct saddle nose deformity (SND) using the new graft technique. SVF was isolated from liposuction aspirate using standard methodology of enzymatic digestion. Two types of BSs were combined with SVF: Bio-Oss granules to create a moldable graft (M-graft), and block-shaped BoneMedik-S to create rigid grafts (R-grafts). The moderate SND was treated using an M-graft. In case of major or complex SND, the nasal dorsum was reconstructed with dorso-columellar L-shaped framework made of R-grafts. The results were evaluated over a period of 6 months to 3 years postoperatively using photogrammetry and FACE-Q appearance appraisal scales. Computerised tomography (CT) scanning of the reconstructed nose and histological analysis of grafted material were also carried out. No complications were observed. The photograms show the restoration of the correct contour of the nose. FACE-Q appraisal scale scores increased significantly, including satisfaction with nose appearance, psychological well-being, and social function. In CT evaluation, there was no substantial resorption or warping of the grafts. Histological findings show osteogenic remodeling of the grafted material. Thus, combining autologous SVF with BSs is a promising strategy for developing rhinoplasty GM.



Keywords

Augmentation rhinoplasty, saddle nose deformity, tissue-engineered bone grafts, stromal vascular fraction

Introduction

Congenital, iatrogenic, and traumatic etiologies can cause a collapse of cartilaginous and bone structures of the external nose and nasal septum, resulting in saddle nose deformity (SND). Other causes are infection (syphilis, leprosy, tuberculosis), inflammatory conditions (polychondritis, Wegener's granulomatosis, sarcoidosis), tumors, and cocaine use. It can also be familial or ethnic [1]. This aesthetic flaw negatively affects the psychological well-being of patients and may be accompanied by breathing impairment [1–3]. Saddle nose is one of the most difficult morpho-functional deformities of the nose to correct, as it entails not only masking with a graft but also planned anatomical reconstruction of all the structures involved [4]. Alloplastic implants, homo- and autografts are traditionally used in patients with different types of SND in order to reestablish facial aesthetic contours and also to reconstruct the nose's structural framework while preserving or restoring the breathing function [5]. Autologous rib cartilage, septal cartilage, and cranial bone remain the preferred grafting materials (GM) for nasal dorsum (ND) augmentation, as they provide the most stable results with a low risk of complications [6]. However, a limited number of autologous tissues available for harvesting, an unpredictable rate of long-term graft resorption, and donor site morbidity represent significant disadvantages of autografting [2, 7, 8]. Alloplastic implants (such as silicone, porous polyethylene, and expanded-polytetrafluoroethylene) and homografts (e.g., irradiated and nonirradiated costal cartilage) can be obtained without additional surgical intervention, but may cause immune rejection, resorption, extrusion, and encapsulation of the inserted items [9, 10]. It has been reported that the traditional management of SND using autologous and homologous costal cartilages produced 22% unsuccessful outcomes with 9% subsequent revision surgery [11]. The search for the optimal GM for augmentation rhinoplasty remains a challenge.

Tissue-engineered bone grafts are currently being actively developed. This group of materials includes items that contain two main components, a bioresorbable scaffold and live cells [12]. The scaffolds support cell attachment and new bone growth (osteoconduction), and in some cases stimulate osteoblast lineage cell differentiation (osteoinduction) [13]. Bioceramics (hydroxyapatite, tricalcium phosphate, bioactive glasses, marine corals, xenogenic bone), biodegradable polymers (collagen, chitosan, polylactic acid, polyglycolic acid, polycaprolactone), and composites (ceramics combined with polymers) have been studied as potential scaffold materials in bone tissue engineering [14, 15]. Each of the listed materials has advantages and disadvantages, and today there is no consensus regarding the "ideal scaffold" [13]. Cells may be combined with osteoconductive biomaterials to enhance their osteogenic capabilities due to differentiation into specialized cells and the production of biologically active substances that promote local osteogenesis [12, 16]. *In vivo* studies, experimental bone defects were treated with scaffolds seeded with different origin stem cells, including bone marrow-derived mesenchymal stem cells (BM-MSCs), adipose tissue-derived mesenchymal stem cells (AT-MSCs), umbilical cord-derived mesenchymal stem cells (MSCs), gingival MSCs, periodontal ligament stem cells, embryonic stem cells (ESCs), and induced pluripotent stem cells (iPSCs) [13, 15]. Promising results of the pre-clinical studies have been demonstrated, but there are considerable limitations to translating some of these technologies to the clinic. For example, manipulations with ESCs remain a topic of great bioethical debate. Both ESCs and iPSCs have a potential tumorigenicity compromising the safety of their clinical use [13]. Reviews of clinical trials have reported successful treatment of nonunion fractures and defects of long bones, cranial defects, mandibular defects, upper jaw bone atrophy, and periodontal defects with tissue-engineered bone grafts [14, 15, 17]. The most commonly clinically applied bioconstructs consist of culture-expanded autologous BM-MSCs and commercially available ceramic-based scaffolds [14, 15]. Bone marrow (BM) tissue is a classic source of multipotent MSCs with osteoblastic lineage differentiation potential; however, BM harvesting is an invasive procedure and yields low numbers of cells [18]. AT-MSCs combined with various scaffolds are an attractive option; the differentiation potential of AT-MSCs is similar to that of other MSCs, and their yield upon isolation and

proliferative rate in culture are higher than those of BM-MSCs [19]. Although numerous experimental studies have yielded promising results, few clinical case reports using AT-MSCs in bone tissue engineering have been published [17, 20–24].

AT-MSCs are part of the stromal vascular fraction (SVF) of adipose tissue, along with a heterogeneous population of many other cell types including preadipocytes, endothelial cells, pericytes, haematopoietic-lineage cells, and fibroblasts [19]. The regenerative features of the SVF are attributed to its paracrine effects. SVF cells secrete vascular endothelial growth factor, hepatocyte growth factor, and transforming growth factor- β in the presence of stimuli such as hypoxia and other growth factors [19], promoting angiogenesis and wound healing and potentially aiding new tissue growth and development [19]. Furthermore, SVF cells augment immunological tolerance by promoting inhibitory macrophages and T-regulatory cells and by decreasing ongoing inflammation [25]. SVF secreted many cytokines or soluble proteins at significantly higher amounts as compared with cultured AT-MSCs, indicating that SVF is a more multifunctional source for cell therapy [26]. The existing literature suggests that angiogenesis, immunomodulation, differentiation, and extracellular matrix secretion are the main avenues through which regeneration and healing are achieved by SVF [27]. Owing to these properties and the ease of harvesting in large amounts with minimal donor-site morbidity, SVF is particularly promising for regenerative therapies [19]. The encouraging results of the use of SVF for the treatment of widespread traumatic calvarial defects [18], replacement of maxillary and mandibular bone defects [28, 29], improving maxillary sinus floor elevation [30], and guided bone regeneration in oral surgery prior to implant placement [31] have been presented in clinical case reports.

This article presents a series of clinical cases of SND treatment using a new GM based on a combination of commercially available bone substitutes (BSs) and autologous SVF.

Case report

Case 1

A 36-year-old man presented with moderate SND. He had a history of a broken nose 6 years ago. The primary rhinoplasty using septal cartilage has already been performed at another clinic and was ineffective due to the rapid resorption of the autograft. A clinical examination revealed saddling and irregularities in the middle third of the ND with a dorsal depression up to 5 mm. No abnormalities were found in the lower third of the nose (Figure 1A–C). The autologous SVF was obtained from the aspirated fat tissue, combined with Bio-Oss granules, and the resulting GM of the moldable consistency (M-graft) was used in rhinoplasty. Six-month postoperative photographs show a smooth ND with correct height (Figure 1D–F).

Case 2

A 25-year-old man presented with congenital major SND. In childhood, a malformed nasal septum was resected to treat nasal obstruction, and conchal cartilages were partially removed during surgery on deformed auricles. The loss of traditional sources of autografts (septal and auricular cartilages) and the patient's refusal of additional surgery for rib cartilage or calvarial bone harvesting contributed to the decision to use the new approach with tissue-engineered grafts. A clinical examination showed a very low, flattened, and broad ND with a dorsal depression of about 8 mm. The tip of the nose was underprojected with a positive septal support test (the tip collapsed when pressed, showing that no tip support was present). The columella was retracted (Figure 2A–C). Two rigid grafts (R-grafts) were created from a BoneMedik-S block containing autologous SVF and were used in open rhinoplasty. A two years follow-up was performed. There were no complications. A slight loss in the height of the ND was detected one year after surgery compared with data six months after surgery. At the last examination, the nose had a fairly aesthetic appearance with subtle concave on the dorsum (Figure 2D–F).

Postoperative three dimensional (3D) computerized tomography (CT) scans showed a two-component construct consisting of dorsal onlay graft and columellar strut graft. No substantial resorption or warping of the grafts was observed (Figure 3).



Figure 1. Case 1. Post-traumatic moderate SND. Secondary rhinoplasty using an M-graft was performed. (A–C) Before surgery; (D–F) six months after surgery



Figure 2. Case 2. Congenital major SND. Rhinoplasty was performed using R-grafts. (A–C) Before surgery; (D–F) two years after surgery

Case 3

A 25-year-old man turned to the department of plastic surgery for the correction of the nasal root and glabella deformity. He had a history of severe craniofacial injury that had occurred two years ago (Figure 4).

After several cranio-maxillofacial surgeries and long-term rehabilitation, the patient returned to social activity, and the issues of facial residual aesthetic flaws became relevant. During a clinical examination, a broad nasal bridge with a wide slit-like excavation extending upward to the glabellar area was recorded. On both sides of the nasal bridge, titanium osteosynthesis plates could be palpated (Figure 5A–C). The replacement of the fronto-nasal bone defect was performed with an M-graft. There were no complications or signs of implant resorption during the 3-year follow-up period. The deformity that bothered the patient was completely eliminated (Figure 5D–F).

Case 4

A 25-year-old woman was admitted to the plastic surgery department with a diagnosis of a complex SND. It is known from the history that the hump of the bony dorsum was congenital, but saddling of the

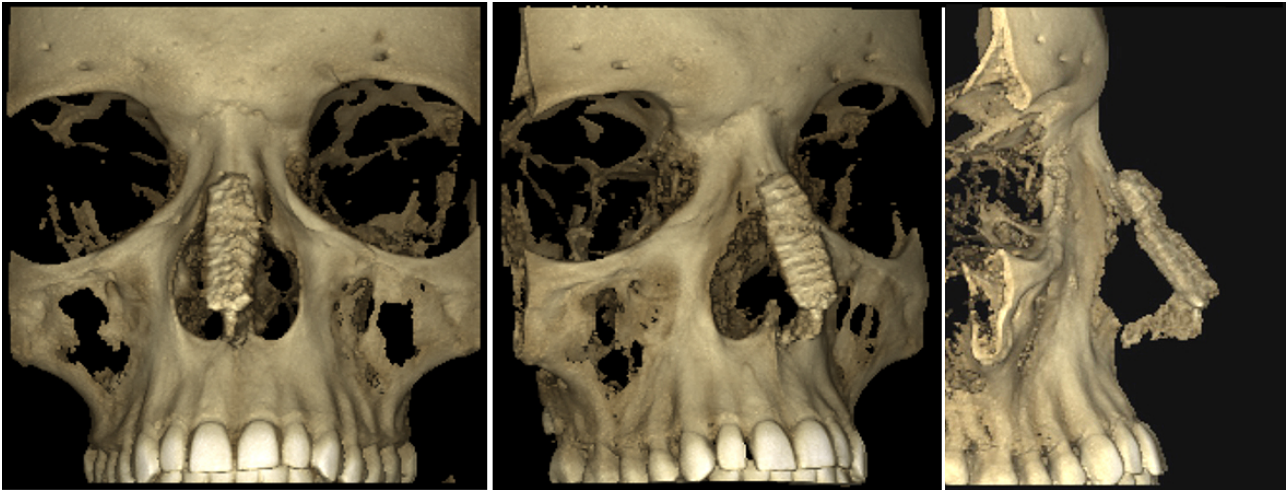


Figure 3. The 3D-CT scans of case 2. Three views of reconstructed saddle nose two years postoperatively: a dorso-caudal support framework made of R-grafts is visible without signs of resorption, deformation, and displacement

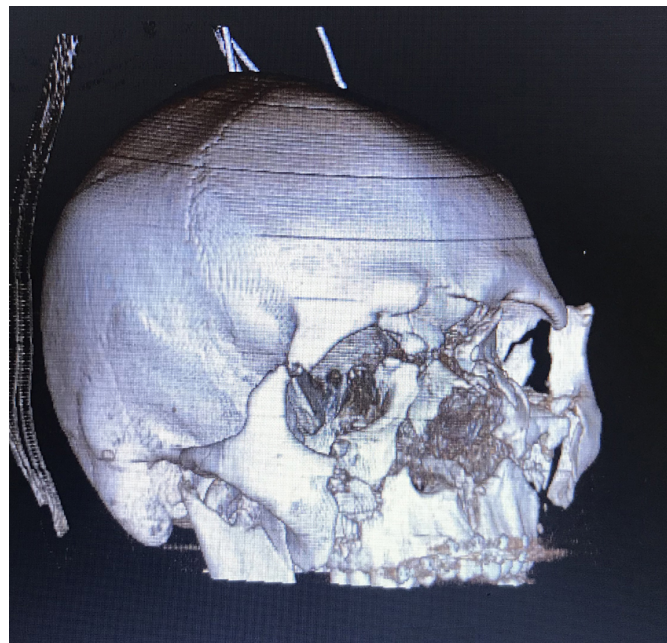


Figure 4. The 3D-CT scans of case 3. Multiple fractures of the maxillofacial bones

cartilaginous dorsum appeared after an unsuccessful septoplasty performed two years ago. The preoperative examination showed a complex of violations including an asymmetric, broad, and protruding bony part of the dorsum, the depressed cartilaginous part of the dorsum, and the drooping tip with retracted columella (Figure 6A–C). Secondary open septorhinoplasty using R-grafts was performed. Six-month postoperative photographs show a modified shape of the nose, a straight, smooth dorsum and improved nasolabial angle (Figure 6D–F).

With the consent of the patient, for the purpose of histological observation, four pieces of R-graft measuring 3 mm × 3 mm × 2 mm were implanted subcutaneously into the retroauricular region (Figure 7).

The patients underwent surgery between May 2012 and September 2019 in the Department of Plastic Surgery of the Chalet Sante Clinic (Krasnodar, Russia). All patients were somatically healthy and had complaints only about the unaesthetic appearance of the nose. The present study includes works on the GM preparation, direct surgical practice, postoperative management of the patient, as well as various diagnostic tests.

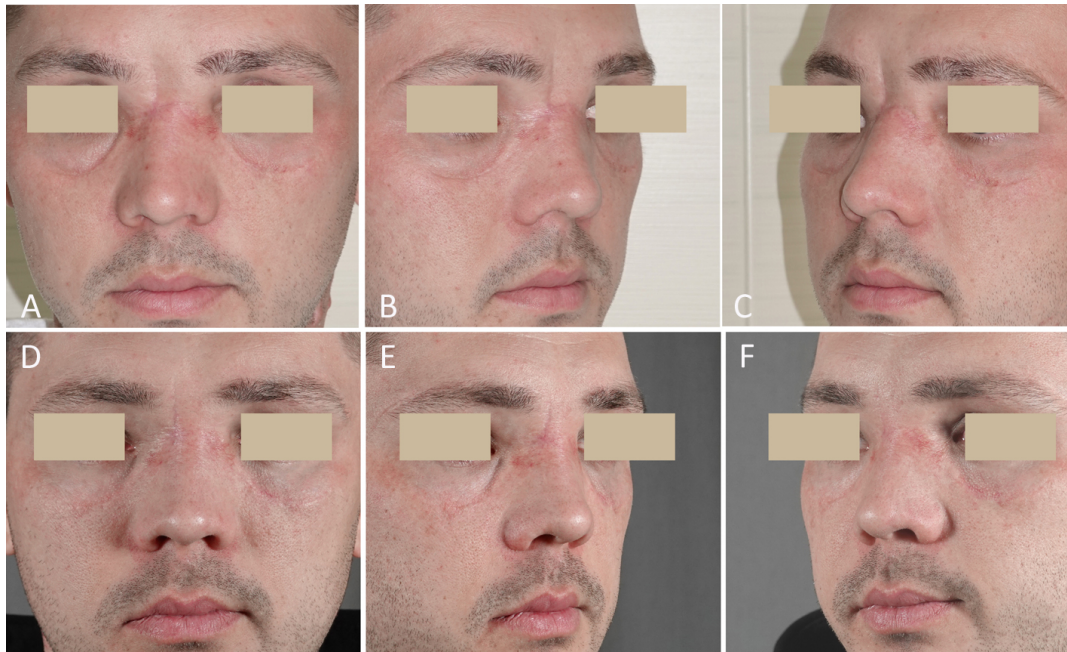


Figure 5. Case 3. Post-traumatic nasal root deformity. Replacement of the bone defect was performed with an M-graft. (A–C) Before surgery; (D–F) three years after surgery



Figure 6. Case 4. Congenital and iatrogenic complex nose deformity. Secondary rhinoplasty was performed using R-grafts. (A–C) Before surgery; (D–F) six months after surgery

Fat harvesting

As the first stage of the surgery, liposuction was performed under local anesthesia to collect adipose tissue. Through small incisions, using a blunt-tip infiltration needle (Byron Medical), 1,000–1,500 mL of a solution containing lidocaine (0.05%) and epinephrine (1:1,000,000) were injected into the subcutaneous fat of the donor site (lower abdomen and/or flanks). After a 10 min exposure, lipoaspiration was performed using a 2.7 mm diameter cannula (Khuori Harvesting Cannula, Wells Jonson) connected to a 60 mL luer-lock syringe until 80–120 mL of adipose tissue was collected. The lipoaspirate was washed twice using a saline solution containing a broadspectrum antibiotic (ceftriaxone 1 g per saline 500 mL). Ten mL of autologous blood serum (ABS) for use in the process of SVF isolation were obtained from the patient's venous blood in accordance with the standard protocol. Small surgical incisions were covered with a sterile adhesive wound dressing. To reduce bruising, a compression abdominal binder was used in the first 5 days after surgery.



Figure 7. Intraoperative views of case 4. (A) R-grafts are in place; (B) micro-incisions in the retroauricular region for the test implantation

Isolation of SVF

In the GMP standard laboratory of Prof. S.V. Ochapovsky Research Institute-Regional Clinical Hospital No. 1 (Krasnodar, Russia), SVF was isolated using the methodology of enzymatic digestion [32]. In each syringe, the volume of washed lipoaspirate in 40–50 mL was adjusted up to 60 mL with a saline solution containing 50 mg of GMP-graded collagenase NB 6 (Nordmark Biochemicals, Germany). A mixture of adipose tissue and collagenase was passed from syringe to syringe through the luer-lock connector back and forth 5 times, transferred into a sterile blood bag, and digested in a water bath at 37°C for 20 min. The resulting suspension was diluted with saline (for reducing viscosity and improving stromal cell sedimentation), distributed in 15 mL test tubes, and fractionated via centrifugation at 3,000 rpm for 20 min. The SVF pellets were collected, washed, and resuspended in 5–10 mL of ABS.

Characterization of SVF

The samples of SVF were tested using an automatic cell counter (Countess, Invitrogen, USA). The number of viable nucleated cells in the SVF portion used in each operation ranged from 40 million to 120 million. The cell surface cluster of differentiation (CD)-antigen profile of SVF cells has been tested as part of separate study [33]. According to immunofluorescence findings, 95–100% of the first passage SVF cells expressed CD13, CD44, CD90, and CD105. A small number of the cells (15–25%) expressed CD31 (endothelial cell marker), c-kit (receptor for stem cell factor SCF and some other progenitor cells), desmin, and smooth muscle actin (muscle cell markers). No CD34-positive cells were detected in the culture (hematopoietic stem cell marker). The cells were synthetically active for extracellular matrix components, such as fibronectin and collagen I (the cells show expression of pro-collagen I, the precursor of type I collagen). The revealed CD profile is commonly reported for identifying adipose-derived stem cells [34].

Combining SVF with BSs and preparing grafts

Two types of BSs were used in combination with SVF, depending on the required mechanical properties of the grafts. If a moldable graft (M-graft) capable of taking a proper shape at the implantation site was required, SVF was combined with granulated BS; if a stable three-dimensional design R-graft was required, the SVF was combined with scaffolds pre-fabricated from block-shaped BS.

To create M-graft, xenogenic Bio-Oss in granules 0.25–1 mm/0.5 g \approx 1 mL (Geistlich Pharma AG, Switzerland) was placed into a test tube with 5 mL of SVF suspension. After 15–30 min of exposure with regular shaking of the tube, centrifugation was carried out (at 1,000 rpm for 4 min), and the supernatant liquid was carefully drained. With the help of a small Volkman spoon, the pellet was transferred into a syringe-applicator (a conventional 1 mL syringe with a cut-off tip). The M-graft is shown in Figure 8.

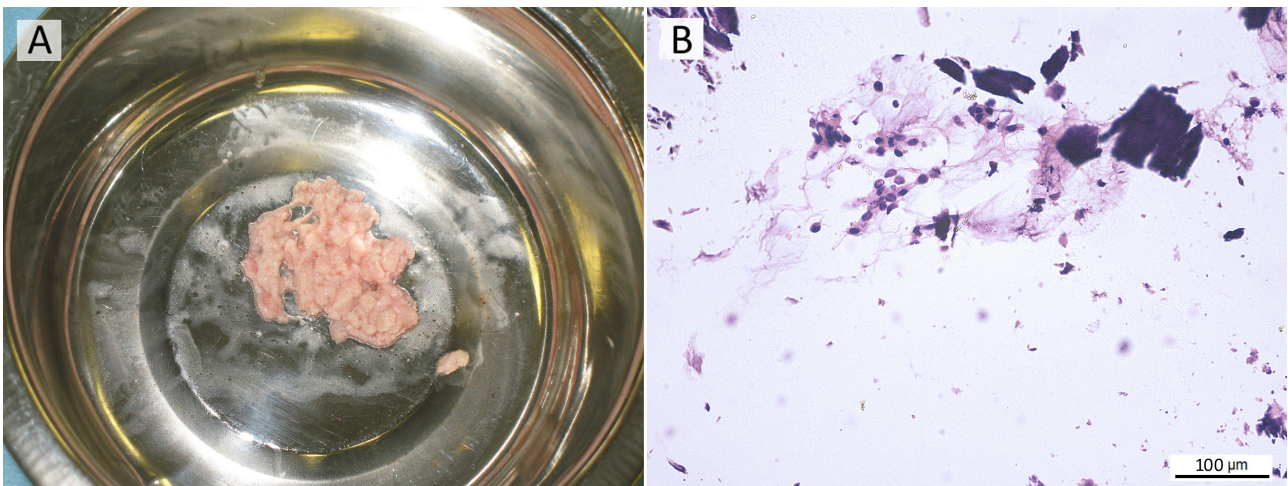


Figure 8. M-graft, a mix of xenogenic Bio-Oss granules with the autologous SVF. (A) M-graft in the form of a shapeless mass of pale pink color on a general view; (B) microparticles of BS are surrounded by a cell-rich fibrous substance of autologous SVF; cytology smear stained with Romanowsky–Giemsa, $\times 200$ magnification

To create R-grafts, based on coral hydroxyapatite BS material BoneMedik-S (Meta Biomed Co, LTD, Korea) in blocks 10 mm \times 10 mm \times 40 mm was used. Two scaffolds, one for the dorsal graft and one for the columellar strut, were cut out of the blocks using a bone microsaw and round bur. The shape and sizes of the scaffolds were determined individually depending on the specifics of the deformation and planned correction. Scaffolds were placed into a test tube with the SVF suspended in 10 mL of the ABS. After 30–60 min of exposure with regular shaking of the tube, porous scaffolds absorbed SVF cells, and the suspension became more transparent. Immediately before use, SVF-containing scaffolds were taken out of the test tube. The suspension was centrifuged, and the resulting residual SVF was applied to the surface of the scaffolds.

Technique of rhinoplasty

The moderate SND with a sufficient projection of the lower third of the nose was corrected using an M-graft (Figure 9A and B). After administration of 2% lidocaine in combination with epinephrine (1:100,000), a sagittal midcolumellar approach was performed, and soft tissues were precisely undermined over the depressed part of the ND. In order to eliminate irregularities and provide proper contact of the graft with the recipient's bed, the ND was rasped. The M-graft was placed into the prepared pocket using a syringe applicator. The midcolumellar incision was sutured with 6-0 Prolene. Then the M-graft was molded externally by hand in order to reproduce the contour of a normal dorsum and stabilized with a thin flexible aluminum nasal splint for 12 days.

In major SND with an underprojected tip and/or retracted columella, the skeletal support of the nose was reconstructed as an L-shaped framework with dorsal and columellar R-grafts (Figure 9C and D). The operation was performed under general anesthesia. The sagittal midcolumellar (case 2) or external transcolumellar approach (case 4) was used to elevate the soft tissue over the nasal tip and dorsum. The ND and caudal septum were treated according to the standard L-shaped framework technique [1]. The columellar strut R-graft was inserted in a pocket between the medial crura and sutured with 5-0 polydioxanone (PDS) to the nasal spine. The dorsal R-graft was then placed on the nasal bones, inserting the proximal end in the subperiosteal pocket. The caudal end of the dorsal graft, superimposed on top of the columellar strut, was sutured to it by several 5-0 PDS sutures. Crus medialis were advanced on the columellar strut and sutured to it with several 5-0 PDS sutures. After the closure of all skin incisions with 6-0 Prolene, external percutaneous and endonasal transfixion sutures with 5-0 Prolene were applied to stabilize the position of the grafts. Packing in the nasal vestibule for 24 h and a light plaster splint for 10 days were used.

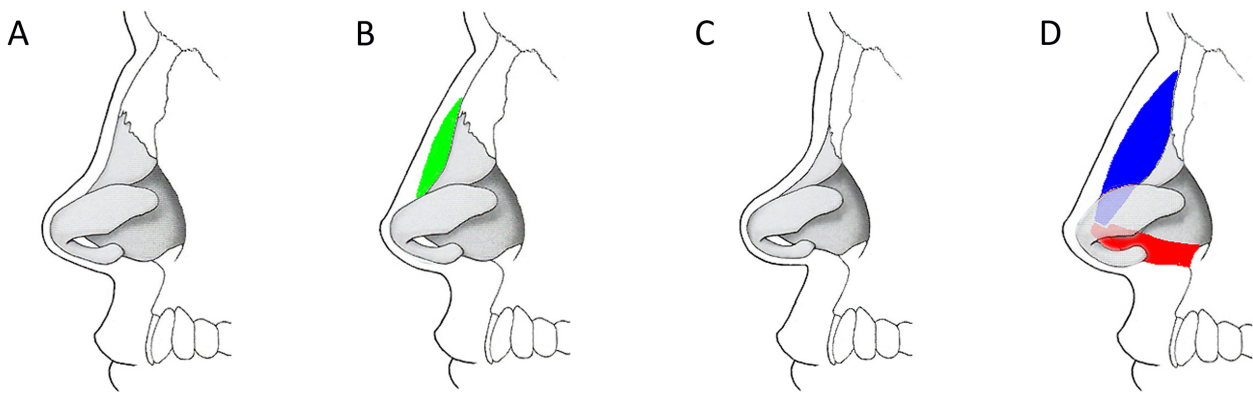


Figure 9. Schematic illustration of the use of grafts at various stages of SND [35]. (A, B) Moderate saddle nose corresponds to a dorsal depression of up to 5 mm, while tip projection and rotation may not be affected; correction is achieved by implantation of M-graft (green) on the depressed part of the ND; (C, D) major saddle nose corresponds to a marked lack of bony and cartilaginous support with a significant loss of the height of the dorsum, decreased projection and cephalic rotation of the tip, retracted columella; skeletal support of the nose is reconstructed using dorsal (blue) and columellar (red) R-grafts

Postoperative care

The patient remained under medical supervision in the clinic for 24 h. Postoperative recommendations included simple instructions for wound care and taking broadspectrum antibiotics for 5 days.

Assessment of results

The results were evaluated over a period of 6 months to 3 years after surgery. Standardized photographs were used to assess nasal contour modifications. Dorsal depression was calculated on profile views as a distance from the most depressed point on the ND contour to the tangential line running from the nasion to the tip. To measure patient-reported outcomes, the FACE-Q scales including satisfaction with the nose, psychological well-being, and social function were utilized. The questionnaires were completed by patients before rhinoplasty and 6 months after it. Each question was answered on a scale of 0 to 4, and the total score was calculated. Higher FACE-Q scores in the form of Rasch-transformed responses represent greater objective values for the subjective variables [36]. In case 2, the reconstructed nasal skeleton was examined using CT scanning (Planmeca, Finland) two years after surgery.

Histological and immunohistochemical analysis

For histological examination, monolayer cytological preparations of M-graft samples were prepared using cytocentrifuge Cytospin-4 (Shandon, UK). The preparations were then stained with Romanowsky-Giemsa [37] and analyzed using an Axiostar microscope (ZEISS, Germany) with a 10× eyepiece and 10×, 20× objectives. Samples of R-graft material obtained 3 months, 6 months, and 24 months after the test implantation were subjected to histological and immunohistochemical analyses. For histological analyses, the harvested specimens were fixed in a 10% neutral buffered paraformaldehyde for 3–5 days, decalcified in a 10% solution of ethylenediaminetetraacetic acid (EDTA) at 37°C, dehydrated through a graded series of ethanol solutions, and then embedded in paraffin. The paraffin sections (5 μm thick) were prepared with a sledge microtome and mounted on the microscope cover glasses. Histological sections were stained with hematoxylin and eosin (HE) for an overview study, and with picrofuchsin according to van Gieson to identify collagenous connective tissue. For immunohistochemical staining, decalcified and paraffin-embedded sections were dewaxed, hydrated, and heat-treated in 1 mmol/L EDTA buffer for antigenic unmasking. Sections were incubated for 60 min at room temperature with a pre-diluted osteopontin polyclonal antibody to identify cellular and interstitial expression. The immunohistochemical study was done on an automatic immunohistostainer (Autostainer Link 48 AS480, Dako, Denmark), using a standard avidin-biotinylated immunoperoxidase technique. For microscopy and digital photography, an Axiostar microscope (ZEISS, Germany) with a 10× eyepiece and 10×, 20×, 40× objectives were used.

Results

The postoperative course was uneventful. At the time of the external splint and sutures removal (10–12 days), the nose had a rather aesthetic appearance without obvious signs of surgical intervention; the augmented ND was painless and stable on palpation. No serious complications, such as inflammation of the implanted material, reaction of the graft covering skin, and violation of the relief of the ND were observed during the up to 3-year follow-up period. An improvement in the aesthetic contours of the nose has been achieved. A comparative analysis of pre- and postoperative photographs revealed an increase of the ND of 3 mm to 7 mm in height, as well as an improvement in the visibility of the initially hidden columella. All patients were satisfied with the aesthetic result of the procedure. FACE-Q appraisal scale scores increased significantly from before to after rhinoplasty, including satisfaction with nose appearance, psychological well-being, and social function. The results are summarized in [Table 1](#).

Table 1. FACE-Q questionnaire results in rasch transformed scores

Appraisal scales		Case 1	Case 2	Case 3	Case 4
Satisfaction with nose	Preoperative	30	10	44	37
	Postoperative	83 (+ 53)	63 (+ 53)	62 (+ 18)	62 (+ 25)
Psychological well-being	Preoperative	30	50	42	38
	Postoperative	95 (+ 65)	63 (+ 13)	50 (+ 12)	62 (+ 24)
Social function	Preoperative	34	52	41	46
	Postoperative	93 (+ 59)	82 (+ 30)	46 (+ 25)	52 (+ 6)

Morphological changes in the implanted R-graft have been shown ([Figure 10](#)). Three months post-implantation, an edging of the newly formed non-mineralized bone matrix, osteoid, was determined around the hydroxyapatite particles. Intermediate spaces were filled with loose cell-rich connective tissue with numerous microvessels. The expression of osteopontin, which is a marker of osteoblastic cell differentiation, confirmed active osteogenesis in the tested material. The specific brown coloring was visualized in the substance of the newly formed bone (NFB), around and within cell-loaded scaffolds, in cells of connective tissue. Six months post-implantation, a significant amount of NFB was determined. Signs of an ongoing osteogenic process were noted as osteoid mass adjacent to partially degraded hydroxyapatite. After van Gieson staining, various stages of bone maturation could be observed, including woven and lamellar NFB. Two years post-implantation, the whole area of histological sections was occupied by mature lamellar bone tissue with lacunae containing viable osteocytes and typical BM spaces. Some residual BS material was still present.

Discussion

The surgical goal of rhinoplasty is to achieve a harmonious, stable shape of the nose with optimal respiratory function. To reach this goal, various regional grafting procedures may be required. Premaxilla augmentation, columellar strut, tip graft, middle third graft, dorsal augmentation, lateral wall graft, and alar graft are commonly used techniques in primary and secondary rhinoplasty [38]. Autologous cartilage derived from various sites depending on the shape and number of grafts required is the most frequently used material for nasal augmentation [39]. While septal, auricular, or costal cartilage grafts have been shown to provide some stability for saddle nose reconstruction, superior outcomes may be achieved using bone grafts [40]. Autologous bone grafts are usually available in sufficient amount and provide adequate structural support to correct any stage of SND [40–42]. Calvarial bone [42–47], iliac crest [41, 48–51], inferior turbinate bone [52, 53], olecranon process [54], vomer [40], and mastoid bone [55] were used as support grafts in rhinoplasty. In most of the subjected publications, favorable aesthetic and functional results with no evidence of bone graft infection, significant resorption, or migration are presented. Some complications on the donor side were described: hematoma [46, 49], seroma [46], long-term donor site morbidity [46], local scalp alopecia [46], bone fracture [54], and artery injury [52].

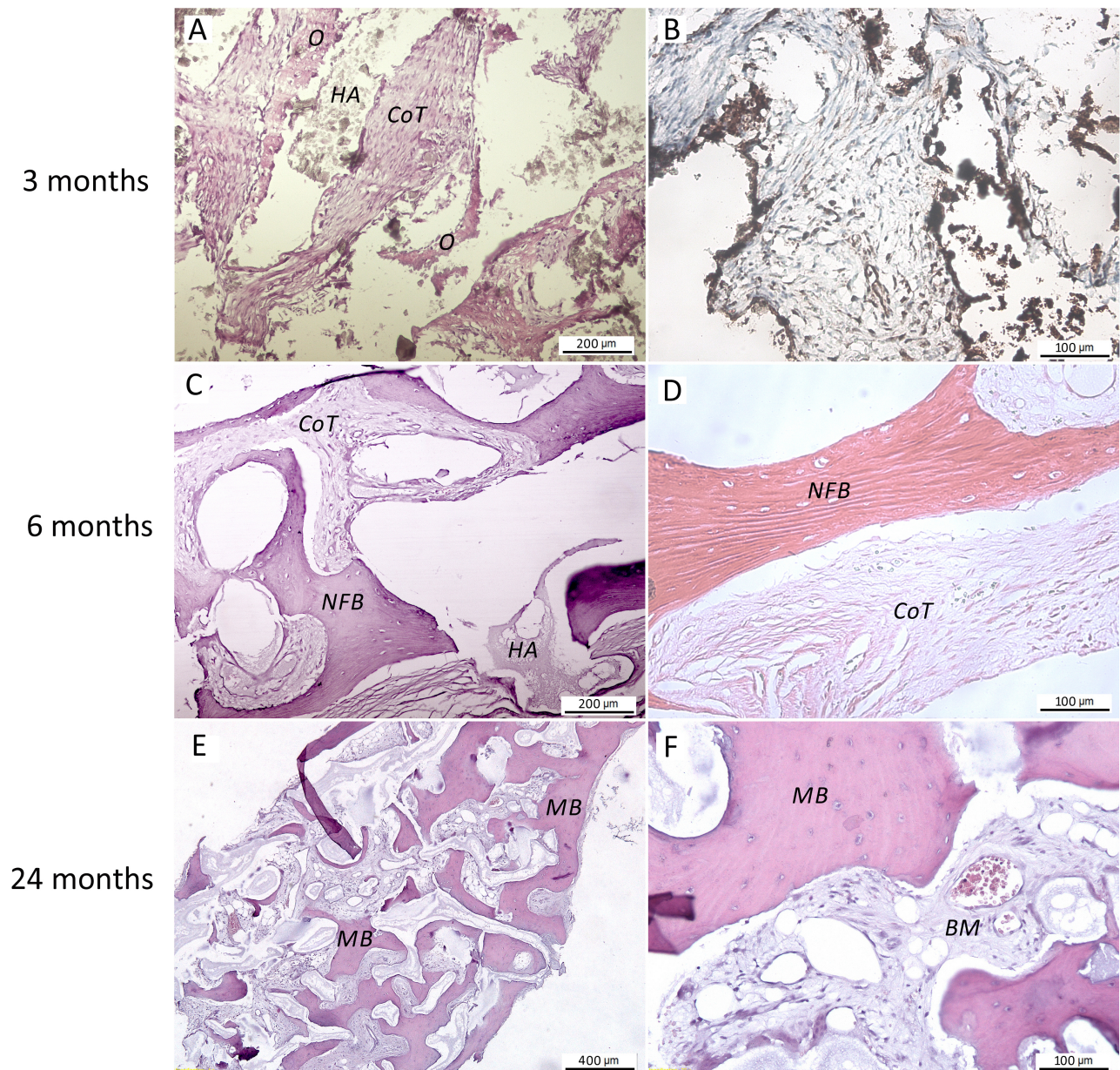


Figure 10. Representative photomicrographs of the coral hydroxyapatite BS material combined with autologous SVF (R-graft) in various post-implantation periods of case 4. A. HE staining, scale bar 200 μm ; B. immunohistochemical staining with anti-osteopontin antibodies, scale bar 100 μm ; C. HE staining, scale bar 200 μm ; D. van Gieson staining, scale bar 100 μm ; (E, F). HE staining, scale bar: 400 μm and 100 μm , respectively. O: osteoid; HA: hydroxyapatite; CoT: connective tissue; NFB: newly formed bone; MB: mature bone

The tissue engineering approach presented in this article avoids the risks of intervention on the donor site and provides reliable support grafts for saddle nose surgery. The absence of any complications during the long-term follow-up indicates the safety of the method. Effectiveness is confirmed by improved measurements of the nasal contour and increased patients' satisfaction with their nose appearance. A slight loss in the height of the ND, detected at the end of the first year of follow-up, may be associated with the final regression of perifocal tissue swelling and minor graft resorption. The control CT scans did not show significant resorption of the grafts 2 years after surgery. Histological findings confirm the successful osteogenic remodeling of the GM.

The grafts are made of commercially available biodegradable BSs as scaffolds and autologous SVF as a cellular component. The SVF isolated from the patient's adipose tissue includes adipose-derived stem/stromal cells, endothelial and smooth muscle cells, macrophages, lymphocytes; the presence of blood cells is possible. Therefore, grafts contain these types of cells. The grafts have suitable mechanical

properties, regenerate bone tissue, and can be obtained in the required amounts without compromising the donor site.

Thus, the combining of autologous SVF with osteoconductive BSs is a promising strategy for developing rhinoplasty GM. These grafts, created in accordance with the principles of tissue engineering, may completely solve the problem of the limited amount and availability of autologous bone grafts. Presented graft technique is less invasive and relatively simple compared to the standard use of autologous bone and cartilage. In certain clinical situations, it may serve as a relevant alternative to traditional methods of auto-, homo-, and alloplasty. Further studies are needed to turn this case series into a reproducible and reliable treatment strategy in augmentation rhinoplasty.

Abbreviations

3D: three dimensional

ABS: autologous blood serum

AT-MSCs: adipose tissue-derived mesenchymal stem cells

BM: bone marrow

BM-MSCs: bone marrow-derived mesenchymal stem cells

BSs: bone substitutes

CD: cluster of differentiation

CT: computerized tomography

ESCs: embryonic stem cells

GM: grafting material

HE: hematoxylin and eosin

M-graft: moldable graft

MSCs: mesenchymal stem cells

ND: nasal dorsum

NFB: newly formed bone

PDS: polydioxanone

R-grafts: rigid grafts

SND: saddle nose deformity

SVF: stromal vascular fraction

Declarations

Author contributions

VK: Conceptualization, Investigation, Methodology, Visualization, Writing—original draft, Writing—review & editing. IG: Investigation, Writing—review & editing. MP: Conceptualization, Writing—review & editing. OP: Investigation, Visualization. All authors read and approved the submitted version.

Conflicts of interest

The authors declare that they have no conflicts of interest.

Ethical approval

The study was conducted according to the guidelines of the Declaration of Helsinki, and approved by the

Local Ethics Committee of the Stavropol State Medical University (Stavropol, Russia). The patients were informed about the procedures in detail. Written consent was obtained from each patient.

Consent to participate

Informed consent to participate in the study was obtained from all participants.

Consent to publication

Informed consent to publication was obtained from relevant participants.

Availability of data and materials

The raw data supporting the conclusions of this manuscript will be made available upon request from the corresponding author.

Funding

Not applicable.

Copyright

© The Author(s) 2024.

References

1. Isac C, Mihajlovic D, Bratu T, Isac A. Severe saddle nose deformity reconstructed with rib cartilage. *Chirurgia (Bucur)*. 2012;107:809–15.
2. Gundeslioglu AO, Yildirim MEC, Yasar S, Uyar I, Ismayilzade M. A different stabilization technique of autogenous cartilage grafts in saddle nose deformity: prevention warping and resorption. *J Craniofac Surg*. 2019;30:811–5.
3. Aboul Wafa AM. Extended L-framework: an innovative technique for reconstruction of low nasal dorsum by autogenous costal cartilage graft. *Plast Reconstr Surg Glob Open*. 2019;7:e2080.
4. Matteo MT. Saddle nose: a systematic approach. In: Farr ST, editor. *Contemporary Rhinoplasty*. Rijeka: IntechOpen Limited; 2018.
5. Pribitkin EA, Ezzat WH. Classification and treatment of the saddle nose deformity. *Otolaryngol Clin North Am*. 2009;42:437–61.
6. Sajjadian A, Rubinstein R, Naghshineh N. Current status of grafts and implants in rhinoplasty: part I. Autologous grafts. *Plast Reconstr Surg*. 2010;125:40e–9e.
7. Wee JH, Park MH, Oh S, Jin HR. Complications associated with autologous rib cartilage use in rhinoplasty: a meta-analysis. *JAMA Facial Plast Surg*. 2015;17:49–55.
8. Lee TY, Lee KI, Dhong ES, Jeong SH, Kim DW, Han SK. Long-term resorption rate of autogenous onlay graft in East Asian rhinoplasty: a retrospective study. *Plast Reconstr Surg*. 2022;149:360–71.
9. Choi JY. Complications of alloplast rhinoplasty and their management: a comprehensive review. *Facial Plast Surg*. 2020;36:517–27.
10. Luan CW, Chen MY, Yan AZ, Tsai YT, Hsieh MC, Yang HY, et al. Complications associated with irradiated homologous costal cartilage use in rhinoplasty: a systematic review and meta-analysis. *J Plast Reconstr Aesthet Surg*. 2022;75:2359–67.
11. Hyun SM, Jang YJ. Treatment outcomes of saddle nose correction. *JAMA Facial Plast Surg*. 2013;15:280–6.
12. Deev RV, Drobyshev AY, Bozo IY, Isaev AA. Ordinary and activated bone grafts: applied classification and the main features. *Biomed Res Int*. 2015;2015:365050.
13. Battafarano G, Rossi M, De Martino V, Marampon F, Borro L, Secinaro A, et al. Strategies for bone regeneration: from graft to tissue engineering. *Int J Mol Sci*. 2021;22:1128.

14. Stammitz S, Klimczak A. Mesenchymal stem cells, bioactive factors, and scaffolds in bone repair: from research perspectives to clinical practice. *Cells*. 2021;10:1925.
15. Venkataiah VS, Yahata Y, Kitagawa A, Inagaki M, Kakiuchi Y, Nakano M, et al. Clinical applications of cell-scaffold constructs for bone regeneration therapy. *Cells*. 2021;10:2687.
16. Gamie Z, Tran GT, Vyzas G, Korres N, Heliotis M, Mantalaris A, et al. Stem cells combined with bone graft substitutes in skeletal tissue engineering. *Expert Opin Biol Ther*. 2012;12:713–29.
17. Song Y, Wang N, Shi H, Zhang D, Wang Q, Guo S, et al. Biomaterials combined with ADSCs for bone tissue engineering: current advances and applications. *Regen Biomater*. 2023;10:rba083.
18. Lendeckel S, Jödicke A, Christophis P, Heidinger K, Wolff J, Fraser JK, et al. Autologous stem cells (adipose) and fibrin glue used to treat widespread traumatic calvarial defects: case report. *J Craniomaxillofac Surg*. 2004;32:370–3.
19. Simonacci F, Bertozzi N, Raposio E. Off-label use of adipose-derived stem cells. *Ann Med Surg (Lond)*. 2017;24:44–51.
20. Thesleff T, Lehtimäki K, Niskakangas T, Huovinen S, Mannerström B, Miettinen S, et al. Cranioplasty with adipose-derived stem cells, beta-tricalcium phosphate granules and supporting mesh: six-year clinical follow-up results. *Stem Cells Transl Med*. 2017;6:1576–82.
21. Sándor GK, Numminen J, Wolff J, Thesleff T, Miettinen A, Tuovinen VJ, et al. Adipose stem cells used to reconstruct 13 cases with cranio-maxillofacial hard-tissue defects. *Stem Cells Transl Med*. 2014;3: 530–40.
22. Mesimäki K, Lindroos B, Törnwall J, Mauno J, Lindqvist C, Kontio R, et al. Novel maxillary reconstruction with ectopic bone formation by GMP adipose stem cells. *Int J Oral Maxillofac Surg*. 2009;38:201–9.
23. Mazzoni E, D’Agostino A, Iaquinta MR, Bononi I, Trevisiol L, Rotondo JC, et al. Hydroxylapatite-collagen hybrid scaffold induces human adipose-derived mesenchymal stem cells to osteogenic differentiation *in vitro* and bone regrowth in patients. *Stem Cells Transl Med*. 2020;9:377–88.
24. Wolff J, Sándor GK, Miettinen A, Tuovinen VJ, Mannerström B, Patrikoski M, et al. GMP-level adipose stem cells combined with computer-aided manufacturing to reconstruct mandibular ameloblastoma resection defects: experience with three cases. *Ann Maxillofac Surg*. 2013;3:114–25.
25. Han S, Sun HM, Hwang KC, Kim SW. Adipose-derived stromal vascular fraction cells: update on clinical utility and efficacy. *Crit Rev Eukaryot Gene Expr*. 2015;25:145–52.
26. Hirose Y, Funahashi Y, Matsukawa Y, Majima T, Yamaguchi M, Kawabata S, et al. Comparison of trophic factors secreted from human adipose-derived stromal vascular fraction with those from adipose-derived stromal/stem cells in the same individuals. *Cytotherapy*. 2018;20:589–91.
27. Guo J, Nguyen A, Banyard DA, Fadavi D, Toranto JD, Wirth GA, et al. Stromal vascular fraction: a regenerative reality? Part 2: mechanisms of regenerative action. *J Plast Reconstr Aesthet Surg*. 2016; 69:180–8.
28. Pellacchia V, Renzi G, Becelli R, Socciarelli F. Bone regeneration of the maxillofacial region through the use of mesenchymal cells obtained by a filtration process of the adipose tissue. *J Craniofac Surg*. 2016; 27:558–60.
29. Manimaran K, Sharma R, Sankaranarayanan S, Perumal SM. Regeneration of mandibular ameloblastoma defect with the help of autologous dental pulp stem cells and buccal pad of fat stromal vascular fraction. *Ann Maxillofac Surg*. 2016;6:97–100.
30. Prins HJ, Schulten EA, Ten Bruggenkate CM, Klein-Nulend J, Helder MN. Bone regeneration using the freshly isolated autologous stromal vascular fraction of adipose tissue in combination with calcium phosphate ceramics. *Stem Cells Transl Med*. 2016;5:1362–74.

31. Solakoglu Ö, Götz W, Kiessling MC, Alt C, Schmitz C, Alt EU. Improved guided bone regeneration by combined application of unmodified, fresh autologous adipose derived regenerative cells and plasma rich in growth factors: a first-in-human case report and literature review. *World J Stem Cells*. 2019;11:124–46.
32. Zhu M, Heydarkhan-Hagvall S, Hedrick M, Benhaim P, Zuk P. Manual isolation of adipose-derived stem cells from human lipoaspirates. *J Vis Exp*. 2013:e50585.
33. Karpyuk V, Perova M, Domenyuk D. Innovation-based approach in reconstruction of reduced jaw alveolar ridge bone using cell regeneration technologies. *Archiv Euromedica*. 2019;9:147–55.
34. Mildmay-White A, Khan W. Cell surface markers on adipose-derived stem cells: a systematic review. *Curr Stem Cell Res Ther*. 2017;12:484–92.
35. Durbec M, Disant F. Saddle nose: classification and therapeutic management. *Eur Ann Otorhinolaryngol Head Neck Dis*. 2014;131:99–106.
36. Soni K, Patro SK, Aneja J, Kaushal D, Goyal A, Shakrawal N. Post-rhinoplasty outcomes in an Indian population assessed using the FACE-Q appraisal scales: a prospective observational study. *J Laryngol Otol*. 2020;134:247–51.
37. Wittekind D, Schulte E, Schmidt G, Frank G. The standard romanowsky-giemsa stain in histology. *Biotech Histochem*. 1991;66:282–95.
38. Vuyk HD, Adamson PA. Biomaterials in rhinoplasty. *Clin Otolaryngol Allied Sci*. 1998;23:209–17.
39. Dresner HS, Hilger PA. An overview of nasal dorsal augmentation. *Semin Plast Surg*. 2008;22:65–73.
40. Gadkaree SK, Weitzman RE, Fuller JC, Justicz N, Gliklich RE. Review of literature of saddle nose deformity reconstruction and presentation of vomer onlay graft. *Laryngoscope Investig Otolaryngol*. 2020;5:1039–43.
41. Cil Y, Ozturk S, Kocman AE, Isik S, Sengezer M. The crooked nose: the use of medial iliac crest bone graft as a supporting framework. *J Craniofac Surg*. 2008;19:1631–8.
42. Paris J, Facon F, Thomassin JM. Saddle nose surgery: long term aesthetic outcomes of support grafts. *Rev Laryngol Otol Rhinol (Bord)*. 2006;127:37–40. French.
43. Emsen IM, Benlier E. Autogenous calvarial bone graft *versus* reconstruction with alloplastic material in treatment of saddle nose deformities: a two-center comparative study. *J Craniofac Surg*. 2008;19:466–75.
44. Himy S, Zink S, Bodin F, Bruant-Rodier C, Wilk A, Meyer C. Calvarial bone grafting in augmentation rhinoplasty. Long-term results. *Rev Stomatol Chir Maxillofac*. 2009;110:256–62. French.
45. Demirtas Y, Yavuzer R, Findikcioglu K, Atabay K, Jackson IT. Fixation of the split calvarial graft in nasal reconstruction. *J Craniofac Surg*. 2006;17:131–8.
46. Cheney ML, Gliklich RE. The use of calvarial bone in nasal reconstruction. *Arch Otolaryngol Head Neck Surg*. 1995;121:643–8.
47. Shipchandler TZ, Chung BJ, Alam DS. Saddle nose deformity reconstruction with a split calvarial bone L-shaped strut. *Arch Facial Plast Surg*. 2008;10:305–11.
48. Ramsay SC, Yeates MG, Ho LC. Bone scanning in the early assessment of nasal bone graft viability. *J Nucl Med*. 1991;32:33–6.
49. Karacaoğlan N, Uysal OA. Use of iliac bone graft for saddle nose deformity. *Auris Nasus Larynx*. 1998;25:49–57.
50. Alshehri WM, Aldosari A, Alherz AH, Alrashood OA, Al Qahtani B. Augmentation rhinoplasty using iliac crest graft in saddle nose deformity. *Cureus*. 2020;12:e9705.
51. Sarukawa S, Sugawara Y, Harii K. Cephalometric long-term follow-up of nasal augmentation using iliac bone graft. *J Craniomaxillofac Surg*. 2004;32:233–5.
52. Ciğer E, İşlek A. Inferior turbinate bone graft for dorsal augmentation in rhinoplasty. *Indian J Otolaryngol Head Neck Surg*. 2022;74:1302–4.

53. Gurlek A, Askar I, Bilen BT, Aydogan H, Fariz A, Alaybeyoglu N. The use of lower turbinate bone grafts in the treatment of saddle nose deformities. *Aesthetic Plast Surg.* 2002;26:407–12.
54. Mehta JS, Zade MP, Nakade DV, Gupta S, Akhila CV. Augmentation rhinoplasty using olecranon bone graft. *Natl J Maxillofac Surg.* 2021;12:344–8.
55. Sadooghi M, Kouhi A. Mastoid bone as a new graft material in rhinoplasty. *Am J Rhinol Allergy.* 2009; 23:e42–6.